Article

Cell Stem Cell

A TIM-3/Gal-9 Autocrine Stimulatory Loop Drives Self-Renewal of Human Myeloid Leukemia Stem Cells and Leukemic Progression

Graphical Abstract

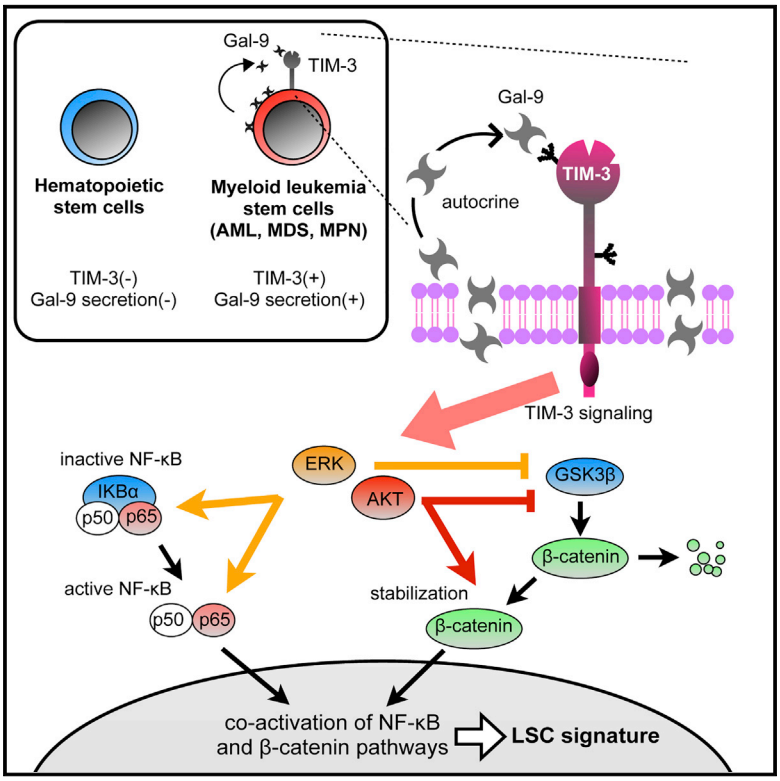

Highlights

- TIM-3+ AML LSCs secrete its ligand galectin-9 in an autocrine manner
- TIM-3/galectin-9 autocrine signaling co-activates NF-κB and β-catenin in LSCs
- This signaling is commonly used by LSCs in most myeloid malignancies

Authors

Yoshikane Kikushige, Toshihiro Miyamoto, Junichiro Yuda, ..., Katsuto Takenaka, Hiromi Iwasaki, Koichi Akashi

Correspondence

akashi@med.kyushu-u.ac.jp

In Brief

Signaling mechanisms specifically active in leukemic stem cells (LSCs) provide therapeutic opportunities. Akashi and colleagues identify a TIM-3/Gal-9 autocrine stimulatory loop that regulates self-renewal of human LSCs, through co-activation of NF-κB and β-catenin signaling, and promotes leukemic progression in a range of myeloid malignancies.

Accession Numbers

GSE62223

Kikushige et al., 2015, Cell Stem Cell *17*, 341–352
September 3, 2015 ©2015 Elsevier Inc.
http://dx.doi.org/10.1016/j.stem.2015.07.011

Cell Stem Cell
Article

A TIM-3/Gal-9 Autocrine Stimulatory Loop Drives Self-Renewal of Human Myeloid Leukemia Stem Cells and Leukemic Progression

Yoshikane Kikushige,[1,2,3] Toshihiro Miyamoto,[1] Junichiro Yuda,[1] Siamak Jabbarzadeh-Tabrizi,[1] Takahiro Shima,[1] Shin-ichiro Takayanagi,[4] Hiroaki Niiro,[1] Ayano Yurino,[1] Kohta Miyawaki,[1] Katsuto Takenaka,[2] Hiromi Iwasaki,[2] and Koichi Akashi[1,2,*]

[1]Department of Medicine and Biosystemic Sciences, Kyushu University Graduate School of Medicine, Fukuoka 812-8582, Japan
[2]Center for Cellular and Molecular Medicine, Kyushu University Hospital, Fukuoka 812-8582, Japan
[3]Japan Society for the Promotion of Science (JSPS), Tokyo 102-0083, Japan
[4]Oncology Research Laboratories, Oncology R&D Unit, R&D Division, Kyowa Hakko Kirin Company, Limited, Tokyo 194-8533, Japan
*Correspondence: akashi@med.kyushu-u.ac.jp
http://dx.doi.org/10.1016/j.stem.2015.07.011

SUMMARY

Signaling mechanisms underlying self-renewal of leukemic stem cells (LSCs) are poorly understood, and identifying pathways specifically active in LSCs could provide opportunities for therapeutic intervention. T-cell immunoglobin mucin-3 (TIM-3) is expressed on the surface of LSCs in many types of human acute myeloid leukemia (AML), but not on hematopoietic stem cells (HSCs). Here, we show that TIM-3 and its ligand, galectin-9 (Gal-9), constitute an autocrine loop critical for LSC self-renewal and development of human AML. Serum Gal-9 levels were significantly elevated in AML patients and in mice xenografted with primary human AML samples, and neutralization of Gal-9 inhibited xenogeneic reconstitution of human AML. Gal-9-mediated stimulation of TIM-3 co-activated NF-κB and β-catenin signaling, pathways known to promote LSC self-renewal. These changes were further associated with leukemic transformation of a variety of pre-leukemic disorders and together highlight that targeting the TIM-3/Gal-9 autocrine loop could be a useful strategy for treating myeloid leukemias.

INTRODUCTION

Acute myeloid leukemia (AML) originates from self-renewing leukemic stem cells (LSCs), and purified human LSCs can repopulate human AML in immunodeficient mice after xenogeneic transplantation (Bonnet and Dick, 1997). In humans, AML LSCs are highly concentrated in the $CD34^+CD38^-$ fraction whose phenotype is analogous to normal hematopoietic stem cells (HSCs), but AML LSCs also have granulocyte/monocyte progenitor (GMP)-like phenotype that are $CD45RA^+CD123^+$ (Yoshimoto et al., 2009). In mouse AML models, LSCs can arise from HSCs as well as from GMPs after introduction of AML-related chimeric fusion genes (Cozzio et al., 2003; Huntly et al., 2004; Krivtsov et al., 2006). LSCs should be an ultimate target for eradication of human AML. Previous studies have reported a number of surface molecules expressed in AML LSCs but not in normal HSCs, including CLL-1 (van Rhenen et al., 2007), CD25 (Saito et al., 2010), CD32 (Saito et al., 2010), and CD96 (Hosen et al., 2007). Recently, we and others have reported that the T-cell immunoglobulin mucin-3 (TIM-3) is expressed on the surface of LSCs in all types of AML by French-American-British (FAB) classification with only exception of M3 (acute promyelocytic leukemia [APL]) (Jan et al., 2011; Kikushige et al., 2010). Because TIM-3 is not expressed in normal human HSCs and because only $TIM\text{-}3^+$ but not $TIM\text{-}3^-$ fraction of human AML cells can reconstitute human AML in immunodeficient mice (Jan et al., 2011; Kikushige et al., 2010), surface TIM-3 should be a strong candidate for therapeutic target. In fact, cytotoxic anti-human TIM-3 antibodies could eradicate human AML LSCs in immunodeficient mice without affecting normal hematopoiesis (Kikushige et al., 2010), suggesting that targeting TIM-3 should be a very promising therapeutic approach for human AML.

TIM-3 is a type 1 cell-surface glycoprotein and was identified originally as a surface molecule expressed in $CD4^+$ Th1 cells in mice (Monney et al., 2002). In human, it is expressed also in a fraction of T cells, NK cells, monocytes, and dendritic cells (DCs) (Anderson et al., 2007; DeKruyff et al., 2010; Gleason et al., 2012; Ndhlovu et al., 2012). Galectin-9 (Gal-9), a ligand of TIM-3, is a β-galactoside binding lectin that contains two carbohydrate recognition domains (CRDs) (Wada and Kanwar, 1997) and binds to N-terminal immunoglobulin variable (IgV) domain of TIM-3 through its two CRDs (Zhu et al., 2005). The function of TIM-3 by Gal-9 ligation has been investigated largely in mouse hematopoiesis. Ligation of TIM-3 by Gal-9 has been shown to phosphorylate tyrosine residues of the cytoplasmic tail of TIM-3 and activate Src family kinases through its Src homology 2 (SH2) binding motif in T cells and monocytes (Anderson et al., 2007; Lee et al., 2011; van de Weyer et al., 2006). TIM-3 signaling induced by Gal-9 ligation exerts pleiotropic effects in immune cells. It induces apoptosis in Th1 cells and negatively regulates the Th1 cell functions (Zhu et al., 2005), whereas in monocytes, its signaling stimulates secretion of tumor necrosis factor-α (TNF-α) and its maturation into DCs (Nagahara et al., 2008), eventually promoting inflammation by innate immunity (Anderson et al., 2007; Kuchroo et al., 2008). It is, however, unknown whether TIM-3 expression in human AML LSCs merely

reflects activation of monocyte-related genes in AML (Kikushige et al., 2010) or whether TIM-3 signaling has a specific function.

Here, we demonstrate evidence that human AML cells secrete a high amount of Gal-9 into patients' sera and that ligation of TIM-3 by Gal-9 activates both NF-κB and β-catenin pathways, presumably to stimulate self-renewal (Schwitalla et al., 2013) of LSCs. Neutralization of human Gal-9 significantly inhibited reconstitution of human AML in immunodeficient mice. Furthermore, upregulation of TIM-3, production of Gal-9, and activation of NF-κB and β-catenin signaling by TIM-3 ligation were always associated not only with primary AML, but also with leukemic transformation from a variety of preleukemic diseases, such as myelodysplastic syndromes (MDSs) and myeloproliferative neoplasms (MPNs), including chronic myelogenous leukemia (CML). Our data suggest that TIM-3 and Gal-9 constitute an essential autocrine stimulatory loop for LSCs to outgrow normal HSCs, presumably representing a universal machinery for development and maintenance of human myeloid malignant stem cells.

RESULTS

Human Gal-9 Is a Ligand for TIM-3 in Primary Human AML Cells

We verified that human Gal-9 binds to the extracellular domain of human TIM-3. To measure the binding activity between human TIM-3 and human Gal-9 proteins, we performed a surface plasmon resonance (SPR) assay by using the Biacore T100 system (GE Healthcare). Human TIM-3-FLAG-Fc proteins were captured on a sensor chip via anti-human IgG antibodies, and then either human recombinant Gal-1, Gal-9, or control buffer was injected to measure changes in the resonance unit. As shown in Figure 1A, Gal-9, but not Gal-1, showed a response against human TIM-3-FLAG-Fc proteins, indicating that Gal-9 physiologically binds to the extracellular domain of human TIM-3.

The clinical characteristics of AML patients analyzed in this study are summarized in Table S1. In 32 of 35 patients, the vast majority of AML LSCs expressed TIM-3 (TIM-3$^+$ AML), whereas the remaining 3 patients, including 1 APL, did not (TIM-3$^-$ AML). We purified the CD34$^+$ AML cells from 5 TIM-3$^+$ AML patients and performed immunoprecipitation-western blot (IP-WB) analysis for human Gal-9. Gal-9 was immunoprecipitated together with TIM-3 in all cases tested, demonstrating that Gal-9 physiologically binds to TIM-3 in primary AML cells (Figure 1B). Thus, Gal-9 should be a ligand for TIM-3 in human as in case of mouse (Zhu et al., 2005).

Primary Human TIM-3$^+$ AML Cells Secrete Gal-9 into the Serum at a High Level

Since primary AML cells had Gal-9 bound to surface TIM-3, we evaluated serum concentration of Gal-9 in TIM-3$^+$ AML patients by an ELISA (Figure 1C). Strikingly, the serum Gal-9 was significantly elevated in 15 AML patients tested. Mean levels of serum Gal-9 were 391.8 pg/ml in AML (n = 15), whereas they were 22.4, 33.5, and 32.3 pg/ml in healthy individuals (n = 12), patients with non-Hodgkin lymphoma (n = 5), and patients with B cell type acute lymphoblastic leukemia (B-ALL) (n = 8), respectively. These data suggest that AML cells themselves secrete Gal-9.

It has been shown that Gal-9 is expressed in various tissues involved in the immune system, including spleen, thymus, and lymphocytes, and in tissues of endodermal origin such as liver, intestine, and lung (Heusschen et al., 2013). Interestingly, both AML LSC (CD34$^+$CD38$^-$) and primitive blast (CD34$^+$CD38$^+$) populations had a high level of intracytoplasmic Gal-9 in all eight AML patients tested (Figure 1D). In normal hematopoiesis, HSCs and hematopoietic progenitor cells (HPCs) had Gal-9 at a similar level (Figure 1E), but the level of intracytoplasmic Gal-9 in AML LSCs was higher than that in normal HSCs (Figure 1F).

Intracytoplasmic Gal-9 does not necessarily mean its secretion because Gal-9 lacks a sequence essential for secretion through ER-Golgi pathway (Hughes, 1999). Prior to secretion, Gal-9 appears as a translocation intermediate through the lipid bilayer of cell membrane (Oomizu et al., 2012). Therefore, Gal-9-secreting cells have Gal-9 on their membrane. To enumerate cells having membrane Gal-9 without detecting Gal-9 bound to surface TIM-3, we stained membrane Gal-9 with an antibody (9M1-3), which specifically recognizes the CRD of Gal-9 that binds the IgV domain of TIM-3. In TIM-3$^+$ AML patients, a considerable population of CD34$^+$CD38$^-$ LSCs and CD34$^+$CD38$^+$ primitive blasts had membrane Gal-9, and its expression declined in CD34$^-$ blasts on fluorescence-activated cell sorting (FACS) analysis (Figures 1G and 1H). In contrast, in a TIM-3$^-$ AML patient, LSCs and primitive blasts did not express membrane Gal-9 (Figure 1G), and in normal hematopoiesis, HSCs, HPCs, T cells, monocytes, B cells, and natural killer (NK) cells (data not shown) did not have membrane Gal-9 at least at the steady state (Figures 1G and 1H). These results strongly suggest that TIM-3$^+$ leukemic stem and blast cells actively secrete Gal-9.

To test whether these AML cells secrete an amount of Gal-9 sufficient to cause elevation of serum Gal-9, we measured Gal-9 concentration in sera from mice reconstituted with human AML. CD34$^+$ blasts from three AML patients, CD34$^+$ lymphoblasts from two B-ALL patients, and three CD34$^+$ cord blood (CB) were transplanted into the NOD.Cg-*Prkdc*^{scid}*Il2rg*^{tm1Wjl}/SzJ (NSG) (Ishikawa et al., 2005) or the C57BL/6.*Rag2*^{null}*Il2rg*^{null}NOD-*Sirpa* (BRGS) strains (Yamauchi et al., 2013). Two months after the xenogeneic transplantation, human cell chimerism reached 10.4%, 86.5%, and 69.2% in average in mice reconstituted with human AML (n = 10), B-ALL (n = 4), and CB (n = 12), respectively. Strikingly, although mice engrafted with human AML cells showed relatively low human cell chimerisms, sera from mice grafted with AML contained a very high level of human Gal-9 (220 pg/ml in average), whereas sera from mice reconstituted with B-ALL or CB cells contained only <20 pg/ml of Gal-9 (Figure 2A). Based on these data, we hypothesized that TIM-3 and Gal-9 constitute a critical autocrine loop to promote maintenance and/or development of AML LSCs.

Inhibition of Gal-9 Binding to TIM-3 Inhibited Reconstitution and Self-Renewal of Human AML LSCs in a Xenogeneic Transplantation Model

To test whether the putative TIM-3/Gal-9 autocrine signaling is critical for function of LSCs, we blocked serum Gal-9 to bind to surface TIM-3 by utilizing a neutralizing Gal-9 antibody (9M1-3) (Klibi et al., 2009; Sada-Ovalle et al., 2012) in xenogeneic hosts. Purified CD34$^+$ cells from four AML cases (patients 2, 14, 26, and 28) were transplanted into irradiated NSG mice.

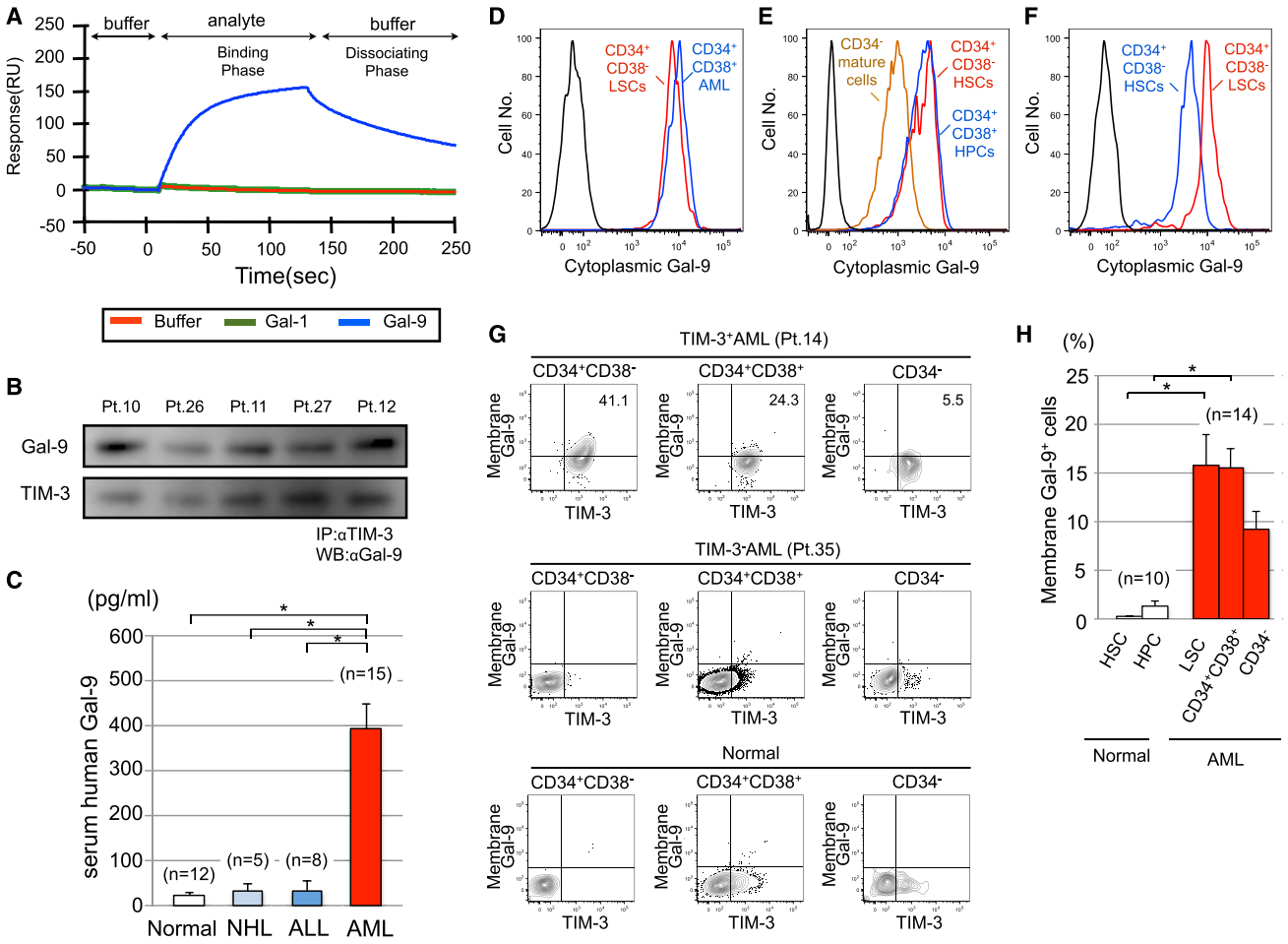

Figure 1. Gal-9, a Ligand for TIM-3, Is Produced from AML LSCs and Primitive AML Cells

(A) Results of the SPR assay by using the Biacore T100 system. Gal-9 but not Gal-1 exhibited a binding phase to human TIM-3-FLAG-Fc protein and then a dissociation phase, indicating physiological binding of Gal-9 to the extracellular domain of human TIM-3.

(B) WB analysis of human Gal-9 after immunoprecipitation of cells from five cases with human AML (patients 10, 11, 12, 26, and 27 in Table S1) by using an anti-human TIM-3 antibody. Gal-9 was co-immunoprecipitated with TIM-3 in all five cases tested.

(C) Serum concentration of Gal-9 measured by ELISA in 15 cases of TIM-3$^+$ AML, and in patients with NHL, B-ALL, and healthy controls.

(D) Intracellular FACS analysis of Gal-9 expression of CD34$^+$CD38$^-$ AML LSCs (red line) and CD34$^+$CD38$^+$ AML cells (blue line). FMO (fluorescence minus one) isotype control (black line) was used to define the negative expression. Representative data from eight independent experiments are shown.

(E) Intracellular FACS analysis of Gal-9 in CD34$^+$CD38$^-$ HSCs (red line), CD34$^+$CD38$^+$ HPCs (blue line), and CD34$^-$ mature cells (yellow line) in normal human hematopoiesis.

(F) Intracellular FACS analysis of Gal-9 in normal HSCs and LSCs from patient 13.

(G) Representative FACS analysis of membrane Gal-9 protein in TIM-3$^+$ AML (patient 14), TIM-3$^-$ AML (patient 35), and normal control.

(H) Summarized data of membrane Gal-9 expression in experiments by using cells from 14 cases with TIM-3$^+$ AML. See also Table S1. Data are represented as mean ± SEM. *$p < 0.05$.

Forty-eight hours after transplantation, 200 μg of a neutralizing anti-human Gal-9 antibody or the same dose of control IgG was intraperitoneally injected once a week for eight times, and then mice were sacrificed. In all four independent experiments, mice injected with control IgG efficiently reconstituted human AML, whereas mice treated with the anti-human Gal-9 antibody exhibited significant reduction of human AML reconstitution and CD34$^+$CD38$^-$ LSC numbers (Figure 2B). Reconstitution of normal hematopoiesis from CB was not affected by the antibody treatment (Figure 2B). These results strongly suggest that blockage of TIM-3/Gal-9 binding impaired human AML reconstitution through inhibiting self-renewing expansion of LSCs.

In order to verify this anti-LSC self-renewal effect of Gal-9 neutralization, we re-transplanted 10^6 hCD34$^+$ AML cells from primary NSG recipients into secondary NSG recipients, and 8 weeks after the secondary transplantation, we evaluated re-engraftment of human AML. In both two independent experiments, all six secondary recipients transplanted with bone marrow (BM) cells from primary recipients treated with control IgG developed AML, whereas none of six mice transplanted with cells from anti-Gal-9 antibody treated primary recipients developed AML (Figure 2C). Thus, anti-Gal-9 antibody treatment effectively eliminated functional LSCs capable of self-renewal in primary recipients.

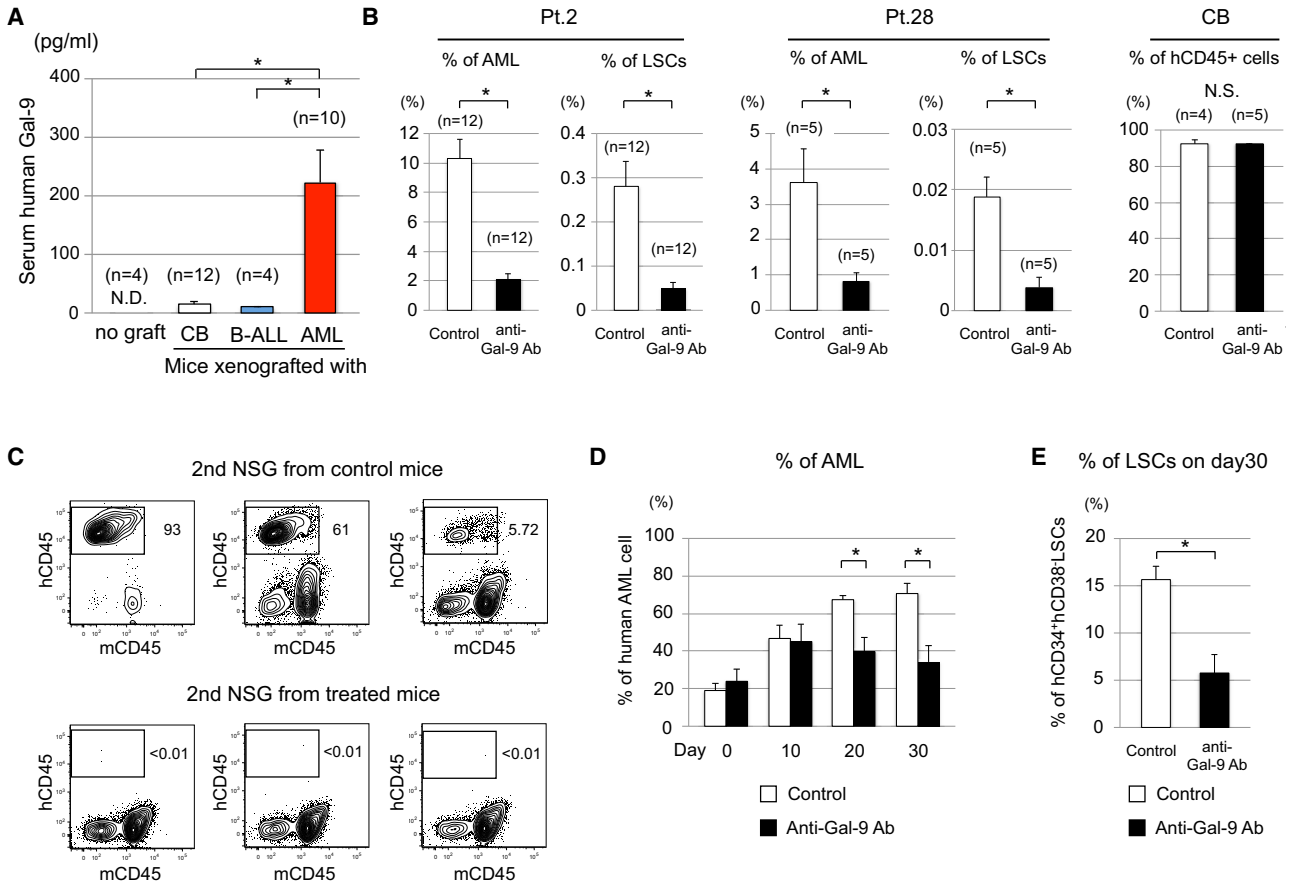

Figure 2. An Autocrine Loop Constituted with TIM-3 and Gal-9 Is Necessary for LSCs to Reconstitute and Self-Renew in a Xenograft Model

(A) Serum human Gal-9 concentration in mice reconstituted with CB, B-ALL, and AML (patients 8, 10, and 14). Note that serum human Gal-9 is elevated only in mice reconstituted with primary AML.

(B) Representative results of Gal-9 neutralization experiments in mice xenografted with human $CD34^+$ AML cells from $TIM\text{-}3^+$ AML patients or with normal CB cells. Injection of an anti-Gal-9 antibody significantly inhibited reconstitution of AML as well as LSCs, but not normal CB reconstitution.

(C) The representative FACS data of secondary NSG recipients transplanted with the residual $hCD34^+$ AML cells purified from primary recipients. Representative results of two independent experiments using cells from patient 2 are shown.

(D) Sequential analysis of circulating human AML burden in mice reconstituted with $TIM\text{-}3^+$ AML (patient 26) after the initiation of Gal-9 neutralization.

(E) Frequencies of $hCD45^+hCD34^+hCD38^-$ LSCs in recipient mice with or without Gal-9 neutralization on day 30. See also Figure S1. Data are represented as mean ± SEM. *$p < 0.05$.

Anti-Human Gal-9 Antibodies Significantly Reduced the Leukemic Burden of Human AML, at Least by Targeting AML LSC Population

We then evaluated whether blocking Gal-9 binding is able to treat human AML in our xenograft model. $CD34^+$ AML cells were transplanted into irradiated NSG mice and 8 weeks after transplantation when successful engraftment of human AML was confirmed by blood sampling, the injection of 500 μg anti-human Gal-9 antibody (9M1-3) was started (day 0) and continued once every 10 days. The change of $hCD45^+$ leukemic burden in blood was serially evaluated. As shown in Figure 2D, after day 20, human AML cells and $CD34^+CD38^-$ LSCs were significantly reduced in mice injected with the anti-Gal-9 antibody, as compared with those injected with control IgG (Figure S1A). Furthermore, on day 30, when mice were sacrificed, the number of $CD34^+CD38^-$ LSCs in anti-Gal-9 antibody-treated mice was significantly lower than that in control mice (Figure 2E). These data strongly suggest that TIM-3 signaling is critical for maintenance of human AML and that reduction of human AML burden was achieved by directly targeting AML LSCs.

Ligation of TIM-3 by Gal-9 Activates NF-κB and β-Catenin Pathways in Primitive Human AML Cells

To clarify the function of TIM-3/Gal-9 interaction in primary AML cells, purified $CD34^+TIM\text{-}3^+$ AML cells were cultured with 500 pg/ml of Gal-9 for 20 hr and were then subjected to cDNA microarray analysis. In all three independent experiments using cells from patients 9, 10, and 29, Gal-9 induced significant changes in the level of gene expression in $CD34^+$ AML blasts. To clarify the signaling pathways that are involved in TIM-3/Gal-9 signaling in AML cells, genes with significant up and downregulation (>2.5-fold and $p < 0.05$) by Gal-9 ligation were subjected to the pathway enrichment analysis based on the WikiPathways (Kelder et al., 2012) using the Genespring

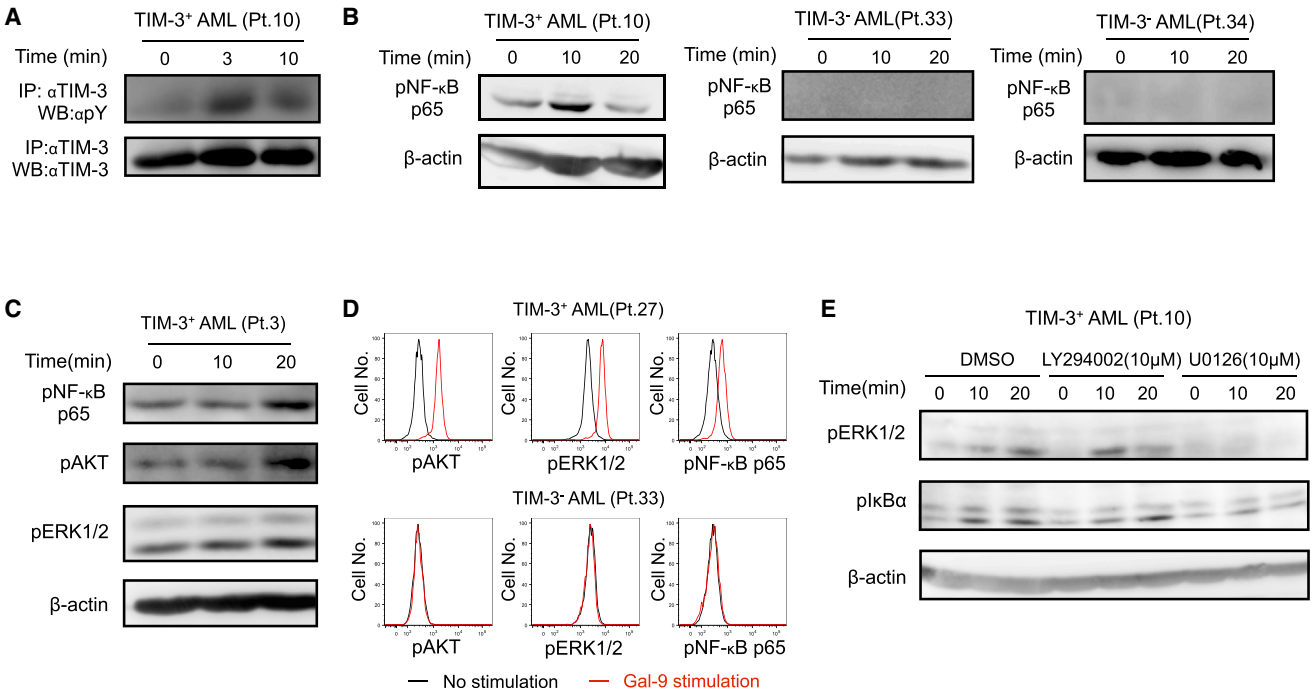

Figure 3. Ligation of TIM-3 by Gal-9 Activates the NF-κB Pathway in Primary AML Cells

(A) Tyrosine phosphorylation of TIM-3 was induced in response to 1.0 ng/ml of Gal-9 in TIM-3$^+$ AML cells. Representative data of three TIM-3$^+$ AML patients tested (patients 10, 26, and 32) are shown.

(B) WB analysis of phosphorylated NF-κB after ligation by 1.0 ng/ml of Gal-9 in primary AML cells. Representative data of TIM-3$^+$ AML cases (patients 2, 3, 10, 12, and 18) are shown. In contrast, phosphorylation of p65 was not induced in TIM-3$^-$ AML cases.

(C) WB analysis of phosphorylated NF-κB, AKT, and ERK after ligation by 5.0 ng/ml of Gal-9 in primary AML cells. Representative data of 4 TIM-3$^+$ AML patients (patients 2, 3, 12, and 18) are shown.

(D) Phosphorylation of AKT, ERK, and p65 was found in cells from 4 TIM-3$^+$ AML cases (patients 11, 12, 26, and 27) 20 min after ligation of TIM-3 by 5.0 ng/ml of Gal-9. Representative results in patient 27 are shown. In contrast, Gal-9 could not induce their phosphorylation in cells from a TIM-3$^-$ AML patient.

(E) Changes in the amount of phosphorylated ERK and IκBα after ligation by 1.0 ng/ml of Gal-9 in the presence of LY294002, an AKT inhibitor, or U0126, a MEK inhibitor. Phosphorylation of ERK or IκBα was inhibited by addition of U0126 but not LY294002. See also Figure S2 and Table S2.

software (Agilent Technologies). The significantly enriched ($p < 0.05$) hematopoietic system or cancer-related pathways are shown in Table S2. Based on these data, we decided to perform detailed analysis of the NF-κB and the Wnt/β-catenin signaling induced by TIM-3 ligation because more than a half of these enriched pathways used NF-κB signaling (Table S2) and because the Wnt/β-catenin signaling pathway is frequently involved in self-renewal of normal and malignant stem cells (Reya et al., 2003; Wang et al., 2010).

Gal-9 Ligation Induces the Phosphorylation of ERK and AKT, Resulting in NF-κB Activation in Primitive Human AML Blasts

It has been shown that ligation of TIM-3 phosphorylates tyrosine residues of the cytoplasmic tail of TIM-3 and activates Src family kinases through its cytoplasmic SH2 binding motif at least in T cells and monocytes (Lee et al., 2011; van de Weyer et al., 2006). First, the tyrosine phosphorylation of TIM-3 following Gal-9 stimulation was evaluated in primary AML cells. Purified CD34$^+$ AML cells were incubated with 1.0 ng/ml of Gal-9, and TIM-3 was immunoprecipitated from cell membrane extracts with an anti-TIM-3 antibody and then blotted with either an anti-phosphotyrosine or anti-TIM-3 antibody. As shown in Figure 3A, ligation of TIM-3 by Gal-9 induced the phosphorylation of its cytoplasmic tyrosine residues of TIM-3 in all 3 TIM-3$^+$ AML cases tested. Furthermore, ligation of TIM-3 by 1.0 ng/ml of Gal-9 also resulted in increased phosphorylation of p65 (RelA) in all five TIM-3$^+$ AML cases tested (Figure 3B). In contrast, in TIM-3$^-$ AML cases, Gal-9 did not induce detectable p65 phosphorylation in leukemic cells (Figure 3B). Consistent with these data, significant nucleus translocation of p65 was observed in CD34$^+$ cells from TIM-3$^+$ AML patients, but not in those from TIM-3$^-$ AML patients (Figure S2).

To identify signaling cascades involved in TIM-3 signaling, changes of phosphorylation status were tested for multiple kinases. Ligation of TIM-3 by Gal-9 in primary TIM-3$^+$ AML cells immediately induced phosphorylation of ERK and AKT, both of which are upstream of the NF-κB pathway (Richmond, 2002) in all four TIM-3$^+$ AML cases tested (Figure 3C). Furthermore, to evaluate phosphorylation status of single AML cells, we performed a Phosflow analysis (BD biosciences). Consistent with results of WB analysis, AKT, ERK1/2 and p65 were significantly phosphorylated by Gal-9 ligation in all four TIM-3$^+$ AML cases tested, but not in cells from a TIM-3$^-$ AML case (Figure 3D). Phosphorylation of IκBα was inhibited partially by addition of U0126, a MEK inhibitor, but not by LY294002, an AKT inhibitor in two independent

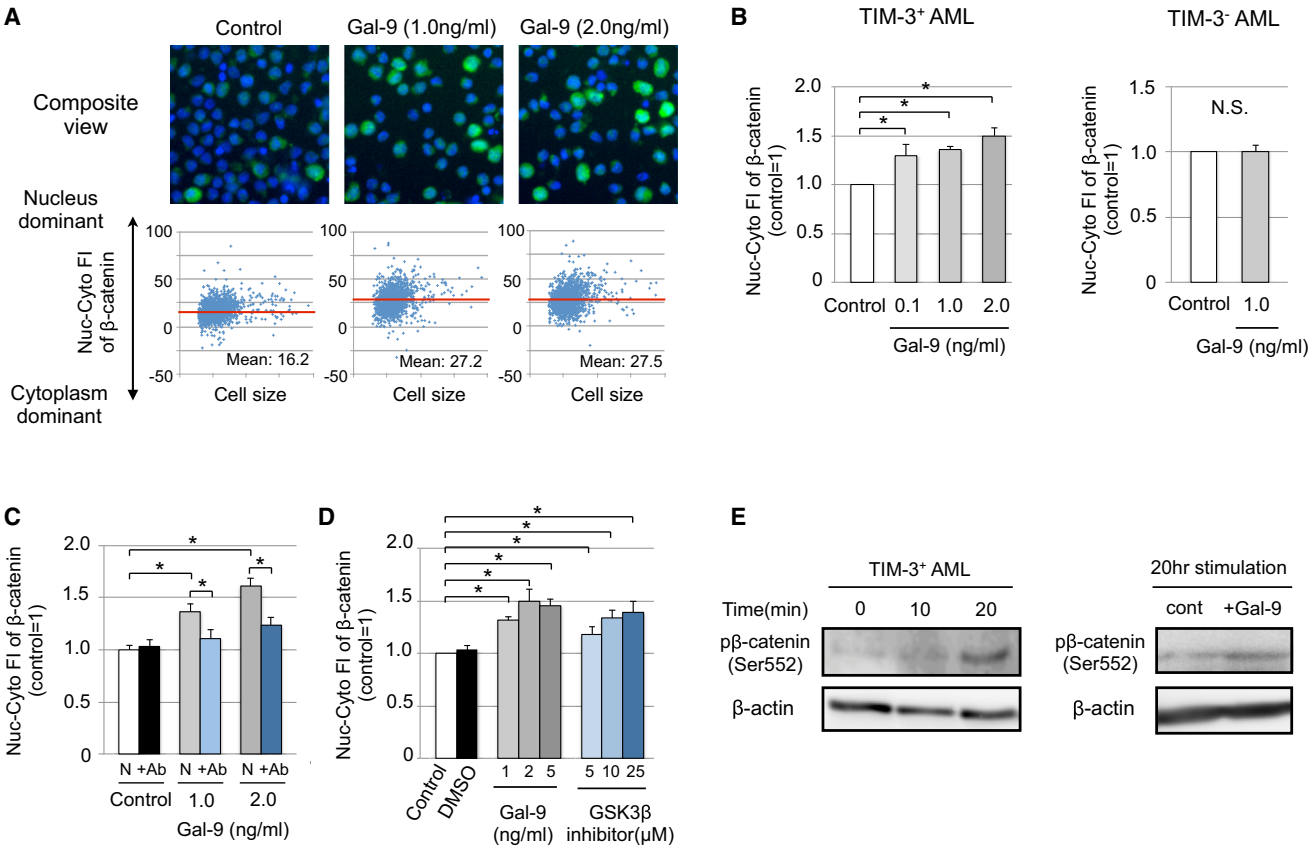

Figure 4. Ligation of TIM-3 by Gal-9 Activates β-Catenin Pathway in Primary AML Cells

(A) Representative results of β-catenin nucleus translocation analysis of primary TIM-3$^+$ AML cells. β-catenin (green) was translocated into the nucleus in response to Gal-9 (upper). Each dot in bottom panels shows cell size and Nuc-Cyto difference of β-catenin fluorescence intensity of single AML cells. Gal-9 stimulation resulted in significant increment of Nuc-Cyto differences.

(B) Summarized data of Nuc-Cyto differences with or without Gal-9 ligation in 9 TIM-3$^+$ AML cases (patients 2, 3, 10, 13, 16, 17, 26, 29, and 32). The translocation was not induced in cells from 3 TIM-3$^-$ AML patients (patients 33, 34, and 35).

(C) The effect of neutralization of Gal-9 by an anti-Gal-9 monoclonal antibody on nucleus translocation of β-catenin. The promotion of β-catenin translocation stimulated by exogenous Gal-9 was cancelled by this treatment in all four independent experiments (patients 2, 10, 13, and 26). Representative data are shown.

(D) β-Catenin nucleus translocation induced by Gal-9 ligation or by incubation with IM-12, a GSK3b inhibitor. In all six independent experiments of TIM-3$^+$ AML cases (patients 2, 3, 10, 13, 26, and 32), the maximum effect of Gal-9 was equal to that of IM-12. Summarized data of six independent experiments are shown.

(E) Induction of β-catenin (Ser552) phosphorylation in TIM-3$^+$ AML (patient 10) by Gal-9 ligation. Data are represented as mean ± SEM. *$p < 0.05$

experiments, indicating that the NF-κB activation by TIM-3 signaling in AML cells is largely dependent on ERK (Figure 3E). These data strongly suggest that TIM-3 signaling in human AML involves both ERK and AKT pathways, and in terms of activation of the NF-κB pathway, the ERK pathway might be critical.

Ligation of TIM-3 by Gal-9 Promotes Nucleus Translocation of β-catenin in Human CD34$^+$ AML Blasts

Activation of the β-catenin pathway is represented by translocation of β-catenin from cytoplasm to nuclei. We quantitated nucleus localization of β-catenin after 20 hr culture of primary CD34$^+$ AML cells with or without Gal-9. To quantitate its intracellular distribution and their translocation of nucleus in single AML cells, we digitized the fluorescence intensity of target molecules in nucleus and cytoplasm of single cells. After a 20-hr culture of purified CD34$^+$ AML cells with or without Gal-9, the difference between nucleus and cytoplasm fluorescence intensity (Nuc-Cyto FI) (Bouck et al., 2011) of β-catenin was measured (Figure S2A).

The difference in Nuc-Cyto FI of β-catenin significantly increased after ligation of TIM-3 by Gal-9 at a concentration of 100 pg/ml to 2 ng/ml in all nine TIM-3$^+$ AML cases tested, but not in TIM3$^-$ AML cases (Figures 4A and 4B). Blocking TIM-3/Gal-9 interaction by the 9M1-3 antibody abrogated this stimulatory effect (Figure 4C). These results indicate that the nucleus translocation of β-catenin occurs in TIM-3$^+$ AML cells in response to the Gal-9 ligation.

GSK3β is a critical inhibitor of the β-catenin pathway by phosphorylating β-catenin to be ubiquitinated and dissolved. TIM-3 signaling can activate the ERK and AKT pathways (Figures 3C and 3D), and both ERK and AKT signaling inhibits GSK3β activity in cancer, resulting in promotion of nucleus translocation of β-catenin (Cross et al., 1995; Ding et al., 2005; Yamaguchi et al., 2012). As shown in Figure 4D, the levels of β-catenin nucleus translocation by addition of Gal-9 were similar to those induced by IM-12, a GSK3β inhibitor (Schmöle et al., 2010) in all six AML cases tested. Furthermore, consistent with the fact

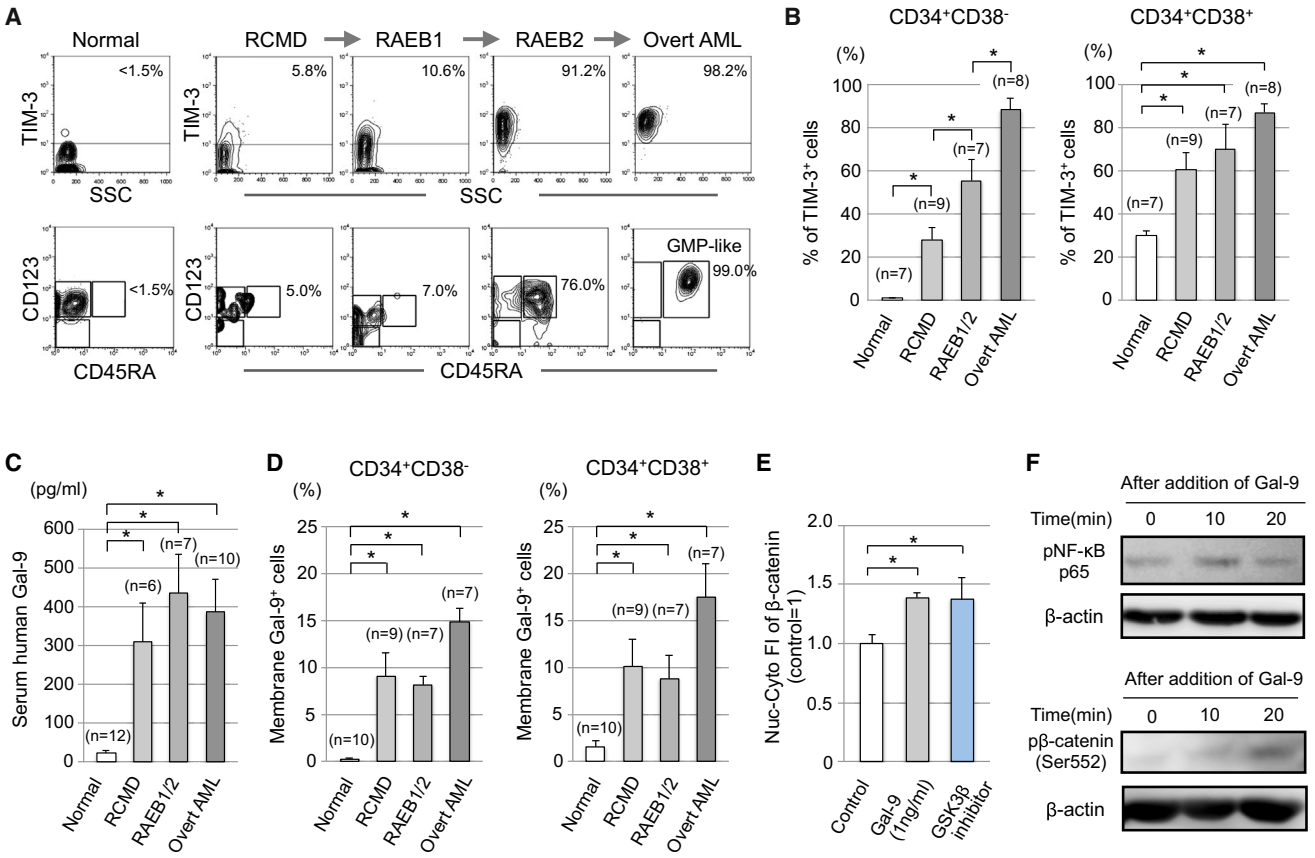

Figure 5. The TIM-3/Gal-9 Autocrine Loop Exists in Patients with MDS

(A) Progressive increase of TIM-3$^+$ cells within the CD34$^+$CD38$^-$ HSC fraction in a RCMD patient who eventually developed overt AML (upper). The CD34$^+$CD38$^-$TIM-3$^+$ population was CD45RA$^+$CD123$^+$, whose phenotype is identical to LSCs in primary AML (bottom).

(B) Percentages of TIM-3$^+$ cells within the CD34$^+$CD38$^-$ and CD34$^+$CD38$^+$ fraction of the bone marrow in each type of MDS cases.

(C) Serum Gal-9 levels in each type of MDS cases. Note that even patients with RCMD had a significantly higher level of serum Gal-9 as compared with normal controls.

(D) Percentages of membrane Gal-9$^+$ cells within the CD34$^+$CD38$^-$ HSC and CD34$^+$CD38$^+$ HPC fractions in each type of MDS. Both populations contain significant numbers of membrane Gal-9$^+$ cells, suggesting that these populations are responsible for secretion of Gal-9.

(E) Nuc-Cyto difference of β-catenin fluorescence intensity of cells from patients with overt AML after ligation with Gal-9 or after incubation with IM-12, a GSK3β inhibitor.

(F) Increases in levels of phosphorylated NF-κB (upper) and phosphorylated β-catenin (bottom) after Gal-9 ligation. Representative data in a patient developed overt AML are shown. Data are represented as mean ± SEM. *$p < 0.05$.

that activated AKT stabilizes β-catenin via phosphorylation of β-catenin at the site of Ser552 (Fang et al., 2007), continuous phosphorylation of this site of β-catenin was seen from 20 min to ~20 hr after ligation of TIM-3 by Gal-9 (Figure 4E). These results suggest that in human AML, TIM-3 signaling activates the β-catenin pathway via AKT and ERK, in addition to the NF-κB pathway via ERK.

The TIM-3/Gal-9 Autocrine Loop Is Used in Myeloid Leukemia Transformed from a Variety of Preleukemic Disorders

Because the NF-κB and β-catenin pathways are frequently involved in a variety of cancers (Reya and Clevers, 2005), we wished to test whether the TIM-3/Gal-9 signaling is used in leukemic transformation in other myeloid malignancies.

Figure 5A shows chronological FACS analyses in a patient with primary MDS of the refractory cytopenia with multilineage dysplasia (RCMD) at diagnosis, who eventually developed overt AML. In this patient, the expression of TIM-3 within the CD34$^+$CD38$^-$ HSC fraction was slightly but significantly elevated at the RCMD stage. TIM-3$^+$ HSCs progressively outgrew TIM-3$^-$ HSCs, as the disease advanced into the refractory anemia with excess of blasts (RAEB) 1, RAEB2, and then overt AML, when virtually all CD34$^+$CD38$^-$ LSCs became TIM-3$^+$. As shown in Figure 5A (bottom), such expanding CD34$^+$CD38$^-$TIM-3$^+$ cells progressively upregulate CD45RA and CD123, becoming analogous to normal GMPs, as LSCs in primary AML do (Yoshimoto et al., 2009). Figure 5B summarized percentages of TIM-3$^+$ cells in the CD34$^+$CD38$^-$ and CD34$^+$CD38$^+$ fraction in 24 MDS patients. The percentages of TIM-3$^+$ cells significantly increased already in RCMD patients and further increased in RAEB and overt AML patients. Serum Gal-9 elevated significantly, reaching >300 pg/ml in average early at the RCMD stage (Figure 5C). Percentages of membrane Gal-9 expressing cells

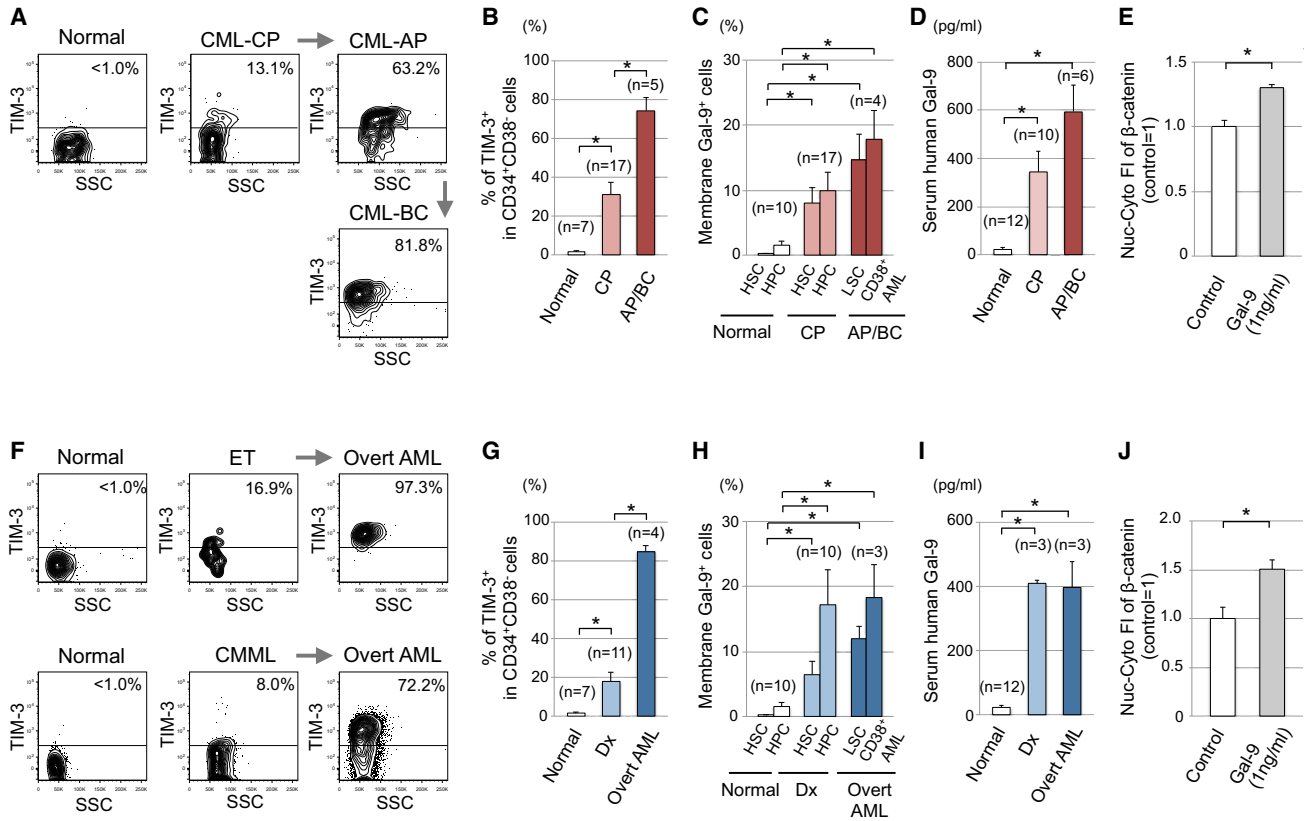

Figure 6. The TIM-3/Gal-9 Autocrine Loop Exists in Patients with MPN

(A) Progressive increase of TIM-3$^+$ cells within the CD34$^+$CD38$^-$ HSC fraction at each stage of human CML.

(B) Percentages of TIM-3$^+$ cells within the CD34$^+$CD38$^-$ fraction of the bone marrow in CML patients at CP or AP/BC phase.

(C) Percentages of membrane Gal-9$^+$ cells within the CD34$^+$CD38$^-$ HSC and the CD34$^+$CD38$^+$ HPC fractions in each clinical phase of CML. Both populations contain significant numbers of membrane Gal-9$^+$ cells even at the CP.

(D) Serum Gal-9 levels in CML patients at the CP or the AP/BC phase. Note that patients at the CP showed a significantly higher level of serum Gal-9 as compared with normal controls.

(E) Gal-9 ligation induced significant nucleus translocation of β-catenin in CD34$^+$ cells from a patient with CML-BC.

(F) Progressive increase of TIM-3$^+$ cells within the CD34$^+$CD38$^-$ HSC fraction in a patient with ET (upper) and with CMML (bottom).

(G) Percentages of TIM-3$^+$ cells within the CD34$^+$CD38$^-$ fraction of the bone marrow in these MPN patients at diagnosis or when they transformed into overt AML.

(H) Percentages of membrane Gal-9$^+$ cells within the CD34$^+$CD38$^-$ HSC and the CD34$^+$CD38$^+$ HPC fractions in ET and CMML patients at diagnosis or when they transformed into overt AML. Both populations contain significant numbers of membrane Gal-9$^+$ cells even at diagnosis.

(I) Serum Gal-9 levels in MPN patients at diagnosis or when they transformed into overt AML.

(J) Gal-9 ligation induced significant nucleus translocation of β-catenin in cells from a patient with CMML. See also Figure S3. Data are represented as mean ± SEM. Dx, diagnosis. *$p < 0.05$.

were also elevated in both CD34$^+$CD38$^-$ and CD34$^+$CD38$^+$ fractions in every stage of MDS (Figure 5D).

Ligation of CD34$^+$TIM-3$^+$ MDS-derived overt AML cells with Gal-9 induced significant elevation of Nuc-Cyto FI of β-catenin in all three cases tested, whose levels were similar to those induced by IM-12, a GSK3β inhibitor (Figure 5E). Ligation by Gal-9 also induced phosphorylation of NF-κB and β-catenin (Figure 5F) in CD34$^+$TIM-3$^+$ overt AML cells, as in primary AML cells did. These data strongly suggest that the TIM-3/Gal-9 autocrine signaling plays a critical role in disease progression of MDS into overt AML.

Similarly, at the chronic phase (CP) of CML patients, the CD34$^+$CD38$^-$ HSC fraction contained ~20% of TIM-3$^+$ cells, and the percentage of TIM-3$^+$ cells within the CD34$^+$CD38$^-$ fraction progressively increased, as disease stages advanced into the accelerated phase (AP) and then the blast crisis (BC), when >80% of CD34$^+$CD38$^-$ LSCs became positive for TIM-3 (Figures 6A and 6B). Significantly high proportions of CD34$^+$CD38$^-$ and CD34$^+$CD38$^+$ populations had membrane Gal-9 in CML patients at every clinical stage (Figure 6C). Serum Gal-9 was also elevated up to ~400 pg/ml at the CP phase and ~600 pg/ml in the AP/BC phases (Figure 6D). Again, CD34$^+$ CML cells at the CP and AP/BC phases incubated with Gal-9 showed increased phosphorylation level of p65, AKT, and ERK (Figures S3A and S3B). Significant nucleus translocation of β-catenin protein was also induced in CD34$^+$ CML cells after Gal-9 stimulation (Figure 6E).

We also checked the expression of TIM-3 in acute leukemia transformation from other MPN, including nine patients with chronic myelomonocytic leukemia (CMML) and six with essential

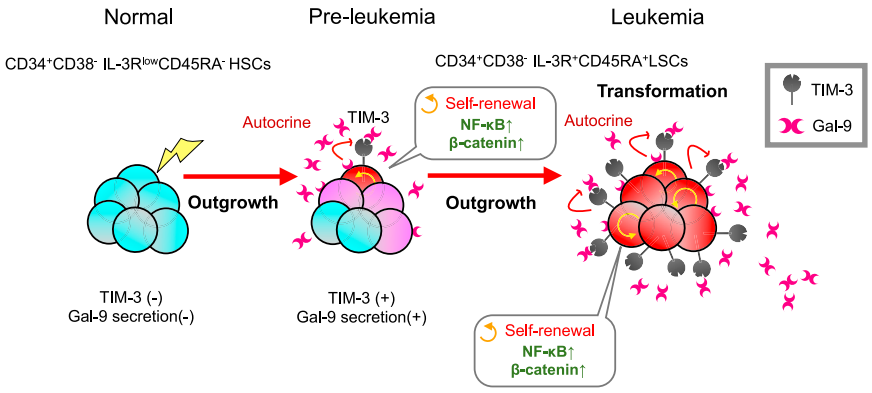

Figure 7. Schema of AML Development Driven by Self-Renewal Signaling of the TIM-3/Gal-9 Autocrine Loop

thrombocythemia (ET). Interestingly, even in these MPN patients at their CP, a small fraction of $CD34^+CD38^-$ HSCs significantly expressed TIM-3, irrespective of primary diagnosis (Figures 6F and 6G). These MPN patients had increased numbers of $CD34^+$ cells expressing membrane Gal-9 (Figure 6H) and elevated serum Gal-9 up to 400 pg/ml (Figure 6I). After transformation into overt AML, the vast majority of $CD34^+CD38^-$ cells became positive for TIM-3, irrespective of their primary diagnosis (Figures 6F and 6G). These cells expressed membrane Gal-9 (Figure 6H), and patients' sera contained high levels of Gal-9 (Figure 6I). TIM-3/Gal-9 interaction again activated NF-κB and β-catenin signaling in $CD34^+$ MPN cells (Figures 6J, S3C, and S3D). Thus, the TIM-3/Gal-9 autocrine signaling appears to be commonly used during development of AML from most types of preleukemic stages in human.

DISCUSSION

Recent genome analysis of myeloid leukemia has shown that sequential acquisition of multiple genetic abnormalities is the principal mechanism for evolution of malignant stem cells to achieve dominant clonal selection (Walter et al., 2012; Welch et al., 2012). These genetic abnormalities progressively accumulate in self-renewing HSCs, and as a consequence of combination of critical driver mutations, these genetically impaired, "preleukemic" HSCs can fully transform into LSCs (Jan et al., 2012; Shlush et al., 2014). During this process, it should be necessary for preleukemic HSCs to outgrow normal HSCs, and finally, they self-renew at a HPC stage such as the GMP to become myeloid LSCs (Krivtsov et al., 2006; Reya et al., 2001; Rossi et al., 2008; Wang et al., 2005). We here propose the TIM-3/Gal-9 autocrine loop as a critical mechanism for such clonal dominancy and self-renewal of LSCs (Figure 7).

We showed evidence that the TIM-3/Gal-9 autocrine loop activates both the NF-κB and the β-catenin signaling in most myeloid leukemias. TIM-3 was originally identified as a protein expressed specifically in LSCs and primitive blasts in human AML but not in normal HSCs (Kikushige et al., 2010). Our study shows that the significant upregulation of TIM-3 in HSC and HPC populations, as well as elevation of serum Gal-9, occurs already in patients with preleukemic myeloid disorders, such as the RCMD stage in MDS, CP, of MPN, including CML. These data suggest that the acquisition of Gal-9 secretion might be one of the early events of leukemia progression. In $TIM\text{-}3^+$ AML patients, Gal-9 is mainly produced by the $CD34^+$ fraction of AML cells that contains LSCs and primitive blasts (Figure 1H). In leukemia transformed from MDS and MPN, Gal-9 was also secreted mainly from $CD34^+$ primitive blast populations (Figures 5D, 6C, 6H, and S3E). Percentages of $TIM\text{-}3^+$ and membrane $Gal\text{-}9^+$ cells progressively increased, as each disease advanced into secondary overt AML (Figures 5 and 6). The ligation of TIM-3 by Gal-9 at concentrations equivalent to patients' serum levels induced simultaneous activation of the NF-κB and β-catenin signaling in leukemia transformed from MDS and MPN (Figures 5, 6, and S3), as well as in de novo AML. These data suggest that the TIM-3/Gal-9 autocrine pathway contributes toward expansion and transformation of malignant myeloid clones.

Since the serum Gal-9 level and percentage of membrane $Gal\text{-}9^+$ cells were upregulated already at early stages of MDS or MPN patients, it is possible that the upregulation of Gal-9 level is an early event prior to the increase of TIM-3 in leukemia cells. It should be critical to elucidate the molecular mechanism of Gal-9 upregulation in future studies. An exome sequence analysis of $TIM\text{-}3^+$ and $TIM\text{-}3^-$ fractions in AML patients has shown that the $TIM\text{-}3^+CD34^+CD38^-$ LSC population represents highly mutated "late" clones, whereas the $TIM\text{-}3^-CD34^+CD38^-$ population consists of less mutated preleukemic HSCs (Jan et al., 2011, 2012). In our analysis, Gal-9 itself did not stimulate the expression of TIM-3 in AML cells at least in vitro (data not shown). These results support our hypothesis that the TIM-3/Gal-9 autocrine signaling plays a critical role in clonal selection, in which preleukemic HSCs progressively outgrow normal HSCs (Figure 7). After leukemic transformation, this pathway becomes essential for LSCs to exert their stem cell function in AML because neutralization of serum human Gal-9 in xenogeneic hosts significantly blocked reconstitution and self-renewal of human AML LSCs (Figure 2). TIM-3/Gal-9 signaling may also be critical for survival of LSCs because we found that deprivation of Gal-9 accelerated apoptotic cell death of LSCs at least in vitro (Figure S1B). Our proposal for scheme of AML progression from HSCs, driven by the TIM-3 and Gal-9 autocrine machinery, is schematized in Figure 7.

Previous studies have proposed that AML cells should be able to stimulate themselves to expand and survive because myeloid leukemic cells can produce cytokines or growth factors, including GM-CSF (Akashi et al., 1991), G-CSF (Murohashi et al., 1989), IL-1β (Oster et al., 1989), IL-6 (Gallipoli blood 2013), and TNF-α (Oster et al., 1989). In fact, cytokine signaling is known to activate NF-κB, and NF-κB signaling is constitutively active in AML LSCs but not in normal HSCs (Guzman et al., 2001). Although such autocrine signaling has been shown to exist in some human leukemias (Akashi et al., 1991), this hypothesis may not be accepted as a fundamental mechanism for growth

or self-renewal of LSCs in AML. For example, a recent report showed that activation of NF-κB pathway in AML occurs independent of autocrine production of cytokines or their receptor mutations such as FLT-3, but it is dependent on activation of Ras pathway (Birkenkamp et al., 2004). In our data, ligation of TIM-3 by Gal-9 in $CD34^+$ AML cells can induce phosphorylation of NF-κB, and consistent with the report, this NF-κB activation occurs via ERK, a signaling molecule downstream of Ras (Figure 3E). Thus, the TIM-3/Gal-9 autocrine loop might be at least one of the critical mechanisms for NF-κB activation in myeloid leukemias.

β-catenin is a key molecule in self-renewing machinery of both normal and malignant HSCs (Reya et al., 2003; Wang et al., 2010). In a mouse AML model, activation of β-catenin pathway is necessary for LSCs to gain self-renewal activity, when mouse non-self-renewing GMP cells were transformed into AML LSCs by retrovirally enforced MLL-AF9 expression (Wang et al., 2010). Primary AML cells constitutively activated this pathway (Simon et al., 2005), and high expression of β-catenin protein in AML cells predicts enhanced colony formation and poor prognosis (Ysebaert et al., 2006). Furthermore, in human CML, accumulation of β-catenin to the nucleus occurs especially in the $CD45RA^+CD123^+$ population of GMP-like phenotype that is finally transformed into LSCs at myeloid BC (Jamieson et al., 2004). Our data show that nucleus translocation of β-catenin occurs in response to Gal-9 in $CD34^+CD38^-CD45RA^+CD123^+$ LSCs not only from primary AML, but also from overt myeloid leukemia progressed from MDS and MPN, including CML. Ligation of TIM-3 by Gal-9 induces phosphorylation of ERK and AKT, whose signaling can inhibit GSK3β, a molecule responsible for degradation of β-catenin by ubiquitination (Yamaguchi et al., 2012). Ligation of TIM-3 also phosphorylates Ser552 of β-catenin for stabilization. Accordingly, TIM-3/Gal-9 signaling might activate the β-catenin pathway via both ERK and AKT in human myeloid leukemias.

The co-activation of NF-κB and β-catenin pathways has been reported to play a cooperative role in conferring cancer-stem-cell properties to non-stem cells in an intestinal cancer model (Schwitalla et al., 2013). In this case, phosphorylated NF-κB binds to β-catenin via CREB-binding protein to strengthen β-catenin transcriptional activities, resulting in generation of strong self-renewal signaling. These data collectively suggest that the TIM-3/Gal-9 autocrine signaling activates both NF-κB and β-catenin pathways to outcompete normal HSCs by promoting self-renewal of LSCs in most types of human myeloid leukemia.

Thus, our data suggest that TIM-3 and Gal-9 constitute a pan-myeloid autocrine loop to develop malignant stem cells in human myeloid malignancies. Signaling molecules downstream of TIM-3 and Gal-9 ligation, as well as surface TIM-3 itself, might be good candidates for cancer stem cell-target therapy common to human myeloid malignancies. Such therapies should be useful not only to eradicate LSCs in AMLs, but also to prevent progression into overt AML in most preleukemic myeloid disorders.

EXPERIMENTAL PROCEDURES

Clinical Samples

The BM, peripheral blood (PB), and serum samples of adult hematological malignancies diagnosed according to World Health Organization (WHO) criteria were enrolled in this study. Table S1 summarizes the primary AML patients' characteristics analyzed in this study. Human adult BM and PB samples were obtained from healthy donors or purchased from AllCells. CB cells were obtained from full-term deliveries (provided by the Kyushu Block Red Cross Blood Center, Japan Red Cross Society). Informed consent was obtained from all patients and controls in accordance with the Helsinki Declaration of 1975 that was revised in 1983. The Institutional Review Board of Kyushu University Hospital approved all research on human subjects.

Purification of AML LSCs and Normal HSCs

For the analyses and sorting of human HSCs and HPCs, cells were stained and sorted by FACS Aria, Aria2, and Aria3 (BD Biosciences). Detailed experimental procedures and antibodies used in the FACS analysis are described in the Supplemental Experimental Procedures.

Surface Plasmon Resonance Assay

The binding of Gal-9 to TIM-3 was analyzed using Biacore T100 system (GE Healthcare). Detailed experimental procedures are described in the Supplemental Experimental Procedures.

Measurement of Serum Gal-9 Concentration

Serum human Gal-9 was measured by using a Human Galectin-9 ELISA kit (KAMIYA Biomedical Company) according to the manufacturer's instructions. We scanned the precoated 96-well plates provided by Multiskan FC (Thermo Fisher Scientific) at a wavelength of 450 nm.

Quantitation for Nucleus Translocation of β-Catenin and p65

Detailed experimental procedures are described in the Supplemental Experimental Procedures.

Xenogeneic Transplantation into Immunodeficient Mice

NSG mice (Ishikawa et al., 2005; Shultz et al., 2005) were purchased from Charles River Laboratories Japan. BRGS mice were developed in our laboratory (Yamauchi et al., 2013). Both mice were bred and housed at Kyushu University. Animal experiments were performed according to the institutional guidelines approved by the animal care committee of Kyushu University. Detailed experimental procedures are described in the Supplemental Experimental Procedures.

Microarray Analysis, Immunoprecipitation, and Western Blot Analysis

Detailed experimental procedures are described in the Supplemental Experimental Procedures.

Statistical Analysis

Data are represented as mean ± SEM. The significance of differences between two groups was determined by Student's t test. p values < 0.05 were considered statistically significant. False discovery rate (FDR)-adjusted p values (q values) were calculated with two-stage sharpened method (Benjamini et al., 2006).

ACCESSION NUMBERS

The microarray data are available in the GEO database under the accession number GEO: GSE62223.

SUPPLEMENTAL INFORMATION

Supplemental Information includes Supplemental Experimental Procedures, three figures, and two tables and can be found with this article online at http://dx.doi.org/10.1016/j.stem.2015.07.011.

AUTHOR CONTRIBUTIONS

Y.K., T.M., and K.A. designed and performed the research, analyzed the data, and wrote the paper. J.Y., S.J.-T., T.S., S.-i.T. H.N., A.Y., K.M., K.T., and H.I. performed the research.

ACKNOWLEDGMENTS

This study was supported in part by a Grant-in-Aid for Young Scientists (A) (to Y.K., no. 26713034), a Grant-in-Aid for Scientific Research on Innovative Areas "Development of Novel Treatment Strategies Targeting Cancer Stem Cells" (to K.A. no., 22130001 and 22130002) and "Stem Cell Aging and Disease" (to T.M., no. 25115002), a Grant-in-Aid for JSPS fellows (to Y.K.), a Grant-in-Aid for Scientific Research (A) (to K.A., no. 25253069), a Grant-in-Aid for Scientific Research (B) (to T.M., no. 23390254), and a Grant-in-Aid from Japan intractable diseases research foundation (to Y.K.). This study was also supported in part by a contribution from Chiyu-Kai and by a grant from Kyowa Hakko Kirin Co., Ltd., and S.-i.T. is an employee of Kyowa Hakko Kirin Co., Ltd.

Received: October 23, 2014
Revised: May 17, 2015
Accepted: July 20, 2015
Published: August 13, 2015

REFERENCES

Akashi, K., Shibuya, T., Harada, M., Takamatsu, Y., Uike, N., Eto, T., and Niho, Y. (1991). Interleukin 4 suppresses the spontaneous growth of chronic myelomonocytic leukemia cells. J. Clin. Invest. *88*, 223–230.

Anderson, A.C., Anderson, D.E., Bregoli, L., Hastings, W.D., Kassam, N., Lei, C., Chandwaskar, R., Karman, J., Su, E.W., Hirashima, M., et al. (2007). Promotion of tissue inflammation by the immune receptor Tim-3 expressed on innate immune cells. Science *318*, 1141–1143.

Benjamini, Y., Krieger, A.M., and Yekutieli, D. (2006). Adaptive linear step-up procedures that control the false discovery rate. Biometrika *93*, 491–507.

Birkenkamp, K.U., Geugien, M., Schepers, H., Westra, J., Lemmink, H.H., and Vellenga, E. (2004). Constitutive NF-kappaB DNA-binding activity in AML is frequently mediated by a Ras/PI3-K/PKB-dependent pathway. Leukemia *18*, 103–112.

Bonnet, D., and Dick, J.E. (1997). Human acute myeloid leukemia is organized as a hierarchy that originates from a primitive hematopoietic cell. Nat. Med. *3*, 730–737.

Bouck, D.C., Shu, P., Cui, J., Shelat, A., and Chen, T. (2011). A high-content screen identifies inhibitors of nuclear export of forkhead transcription factors. J. Biomol. Screen. *16*, 394–404.

Cozzio, A., Passegué, E., Ayton, P.M., Karsunky, H., Cleary, M.L., and Weissman, I.L. (2003). Similar MLL-associated leukemias arising from self-renewing stem cells and short-lived myeloid progenitors. Genes Dev. *17*, 3029–3035.

Cross, D.A., Alessi, D.R., Cohen, P., Andjelkovich, M., and Hemmings, B.A. (1995). Inhibition of glycogen synthase kinase-3 by insulin mediated by protein kinase B. Nature *378*, 785–789.

DeKruyff, R.H., Bu, X., Ballesteros, A., Santiago, C., Chim, Y.L., Lee, H.H., Karisola, P., Pichavant, M., Kaplan, G.G., Umetsu, D.T., et al. (2010). T cell/transmembrane, Ig, and mucin-3 allelic variants differentially recognize phosphatidylserine and mediate phagocytosis of apoptotic cells. J. Immunol. *184*, 1918–1930.

Ding, Q., Xia, W., Liu, J.C., Yang, J.Y., Lee, D.F., Xia, J., Bartholomeusz, G., Li, Y., Pan, Y., Li, Z., et al. (2005). Erk associates with and primes GSK-3beta for its inactivation resulting in upregulation of beta-catenin. Mol. Cell *19*, 159–170.

Fang, D., Hawke, D., Zheng, Y., Xia, Y., Meisenhelder, J., Nika, H., Mills, G.B., Kobayashi, R., Hunter, T., and Lu, Z. (2007). Phosphorylation of beta-catenin by AKT promotes beta-catenin transcriptional activity. J. Biol. Chem. *282*, 11221–11229.

Gleason, M.K., Lenvik, T.R., McCullar, V., Felices, M., O'Brien, M.S., Cooley, S.A., Verneris, M.R., Cichocki, F., Holman, C.J., Panoskaltsis-Mortari, A., et al. (2012). Tim-3 is an inducible human natural killer cell receptor that enhances interferon gamma production in response to galectin-9. Blood *119*, 3064–3072.

Guzman, M.L., Neering, S.J., Upchurch, D., Grimes, B., Howard, D.S., Rizzieri, D.A., Luger, S.M., and Jordan, C.T. (2001). Nuclear factor-kappaB is constitutively activated in primitive human acute myelogenous leukemia cells. Blood *98*, 2301–2307.

Heusschen, R., Griffioen, A.W., and Thijssen, V.L. (2013). Galectin-9 in tumor biology: a jack of multiple trades. Biochim. Biophys. Acta *1836*, 177–185.

Hosen, N., Park, C.Y., Tatsumi, N., Oji, Y., Sugiyama, H., Gramatzki, M., Krensky, A.M., and Weissman, I.L. (2007). CD96 is a leukemic stem cell-specific marker in human acute myeloid leukemia. Proc. Natl. Acad. Sci. USA *104*, 11008–11013.

Hughes, R.C. (1999). Secretion of the galectin family of mammalian carbohydrate-binding proteins. Biochim. Biophys. Acta *1473*, 172–185.

Huntly, B.J., Shigematsu, H., Deguchi, K., Lee, B.H., Mizuno, S., Duclos, N., Rowan, R., Amaral, S., Curley, D., Williams, I.R., et al. (2004). MOZ-TIF2, but not BCR-ABL, confers properties of leukemic stem cells to committed murine hematopoietic progenitors. Cancer Cell *6*, 587–596.

Ishikawa, F., Yasukawa, M., Lyons, B., Yoshida, S., Miyamoto, T., Yoshimoto, G., Watanabe, T., Akashi, K., Shultz, L.D., and Harada, M. (2005). Development of functional human blood and immune systems in NOD/SCID/IL2 receptor gamma chain(null) mice. Blood *106*, 1565–1573.

Jamieson, C.H., Ailles, L.E., Dylla, S.J., Muijtjens, M., Jones, C., Zehnder, J.L., Gotlib, J., Li, K., Manz, M.G., Keating, A., et al. (2004). Granulocyte-macrophage progenitors as candidate leukemic stem cells in blast-crisis CML. N. Engl. J. Med. *351*, 657–667.

Jan, M., Chao, M.P., Cha, A.C., Alizadeh, A.A., Gentles, A.J., Weissman, I.L., and Majeti, R. (2011). Prospective separation of normal and leukemic stem cells based on differential expression of TIM3, a human acute myeloid leukemia stem cell marker. Proc. Natl. Acad. Sci. USA *108*, 5009–5014.

Jan, M., Snyder, T.M., Corces-Zimmerman, M.R., Vyas, P., Weissman, I.L., Quake, S.R., and Majeti, R. (2012). Clonal evolution of preleukemic hematopoietic stem cells precedes human acute myeloid leukemia. Sci. Transl. Med. *4*, 149ra118.

Kelder, T., van Iersel, M.P., Hanspers, K., Kutmon, M., Conklin, B.R., Evelo, C.T., and Pico, A.R. (2012). WikiPathways: building research communities on biological pathways. Nucleic Acids Res. *40*, D1301–D1307.

Kikushige, Y., Shima, T., Takayanagi, S., Urata, S., Miyamoto, T., Iwasaki, H., Takenaka, K., Teshima, T., Tanaka, T., Inagaki, Y., and Akashi, K. (2010). TIM-3 is a promising target to selectively kill acute myeloid leukemia stem cells. Cell Stem Cell *7*, 708–717.

Klibi, J., Niki, T., Riedel, A., Pioche-Durieu, C., Souquere, S., Rubinstein, E., Le Moulec, S., Guigay, J., Hirashima, M., Guemira, F., et al. (2009). Blood diffusion and Th1-suppressive effects of galectin-9-containing exosomes released by Epstein-Barr virus-infected nasopharyngeal carcinoma cells. Blood *113*, 1957–1966.

Krivtsov, A.V., Twomey, D., Feng, Z., Stubbs, M.C., Wang, Y., Faber, J., Levine, J.E., Wang, J., Hahn, W.C., Gilliland, D.G., et al. (2006). Transformation from committed progenitor to leukaemia stem cell initiated by MLL-AF9. Nature *442*, 818–822.

Kuchroo, V.K., Dardalhon, V., Xiao, S., and Anderson, A.C. (2008). New roles for TIM family members in immune regulation. Nat. Rev. Immunol. *8*, 577–580.

Lee, J., Su, E.W., Zhu, C., Hainline, S., Phuah, J., Moroco, J.A., Smithgall, T.E., Kuchroo, V.K., and Kane, L.P. (2011). Phosphotyrosine-dependent coupling of Tim-3 to T-cell receptor signaling pathways. Mol. Cell. Biol. *31*, 3963–3974.

Monney, L., Sabatos, C.A., Gaglia, J.L., Ryu, A., Waldner, H., Chernova, T., Manning, S., Greenfield, E.A., Coyle, A.J., Sobel, R.A., et al. (2002). Th1-specific cell surface protein Tim-3 regulates macrophage activation and severity of an autoimmune disease. Nature *415*, 536–541.

Murohashi, I., Tohda, S., Suzuki, T., Nagata, K., Yamashita, Y., and Nara, N. (1989). Autocrine growth mechanisms of the progenitors of blast cells in acute myeloblastic leukemia. Blood *74*, 35–41.

Nagahara, K., Arikawa, T., Oomizu, S., Kontani, K., Nobumoto, A., Tateno, H., Watanabe, K., Niki, T., Katoh, S., Miyake, M., et al. (2008). Galectin-9 increases Tim-3+ dendritic cells and CD8+ T cells and enhances antitumor immunity via galectin-9-Tim-3 interactions. J. Immunol. *181*, 7660–7669.

Ndhlovu, L.C., Lopez-Vergès, S., Barbour, J.D., Jones, R.B., Jha, A.R., Long, B.R., Schoeffler, E.C., Fujita, T., Nixon, D.F., and Lanier, L.L. (2012). Tim-3

marks human natural killer cell maturation and suppresses cell-mediated cytotoxicity. Blood *119*, 3734–3743.

Oomizu, S., Arikawa, T., Niki, T., Kadowaki, T., Ueno, M., Nishi, N., Yamauchi, A., Hattori, T., Masaki, T., and Hirashima, M. (2012). Cell surface galectin-9 expressing Th cells regulate Th17 and Foxp3+ Treg development by galectin-9 secretion. PLoS ONE *7*, e48574.

Oster, W., Cicco, N.A., Klein, H., Hirano, T., Kishimoto, T., Lindemann, A., Mertelsmann, R.H., and Herrmann, F. (1989). Participation of the cytokines interleukin 6, tumor necrosis factor-alpha, and interleukin 1-beta secreted by acute myelogenous leukemia blasts in autocrine and paracrine leukemia growth control. J. Clin. Invest. *84*, 451–457.

Reya, T., and Clevers, H. (2005). Wnt signalling in stem cells and cancer. Nature *434*, 843–850.

Reya, T., Morrison, S.J., Clarke, M.F., and Weissman, I.L. (2001). Stem cells, cancer, and cancer stem cells. Nature *414*, 105–111.

Reya, T., Duncan, A.W., Ailles, L., Domen, J., Scherer, D.C., Willert, K., Hintz, L., Nusse, R., and Weissman, I.L. (2003). A role for Wnt signalling in self-renewal of haematopoietic stem cells. Nature *423*, 409–414.

Richmond, A. (2002). Nf-kappa B, chemokine gene transcription and tumour growth. Nat. Rev. Immunol. *2*, 664–674.

Rossi, D.J., Jamieson, C.H., and Weissman, I.L. (2008). Stems cells and the pathways to aging and cancer. Cell *132*, 681–696.

Sada-Ovalle, I., Chávez-Galán, L., Torre-Bouscoulet, L., Nava-Gamiño, L., Barrera, L., Jayaraman, P., Torres-Rojas, M., Salazar-Lezama, M.A., and Behar, S.M. (2012). The Tim3-galectin 9 pathway induces antibacterial activity in human macrophages infected with Mycobacterium tuberculosis. J. Immunol. *189*, 5896–5902.

Saito, Y., Kitamura, H., Hijikata, A., Tomizawa-Murasawa, M., Tanaka, S., Takagi, S., Uchida, N., Suzuki, N., Sone, A., Najima, Y., et al. (2010). Identification of therapeutic targets for quiescent, chemotherapy-resistant human leukemia stem cells. Sci. Transl. Med. *2*, 17ra9.

Schmöle, A.C., Brennführer, A., Karapetyan, G., Jaster, R., Pews-Davtyan, A., Hübner, R., Ortinau, S., Beller, M., Rolfs, A., and Frech, M.J. (2010). Novel indolylmaleimide acts as GSK-3beta inhibitor in human neural progenitor cells. Bioorg. Med. Chem. *18*, 6785–6795.

Schwitalla, S., Fingerle, A.A., Cammareri, P., Nebelsiek, T., Göktuna, S.I., Ziegler, P.K., Canli, O., Heijmans, J., Huels, D.J., Moreaux, G., et al. (2013). Intestinal tumorigenesis initiated by dedifferentiation and acquisition of stem-cell-like properties. Cell *152*, 25–38.

Shlush, L.I., Zandi, S., Mitchell, A., Chen, W.C., Brandwein, J.M., Gupta, V., Kennedy, J.A., Schimmer, A.D., Schuh, A.C., Yee, K.W., et al.; HALT Pan-Leukemia Gene Panel Consortium (2014). Identification of pre-leukaemic haematopoietic stem cells in acute leukaemia. Nature *506*, 328–333.

Shultz, L.D., Lyons, B.L., Burzenski, L.M., Gott, B., Chen, X., Chaleff, S., Kotb, M., Gillies, S.D., King, M., Mangada, J., et al. (2005). Human lymphoid and myeloid cell development in NOD/LtSz-scid IL2R gamma null mice engrafted with mobilized human hemopoietic stem cells. J. Immunol. *174*, 6477–6489.

Simon, M., Grandage, V.L., Linch, D.C., and Khwaja, A. (2005). Constitutive activation of the Wnt/beta-catenin signalling pathway in acute myeloid leukaemia. Oncogene *24*, 2410–2420.

van de Weyer, P.S., Muehlfeit, M., Klose, C., Bonventre, J.V., Walz, G., and Kuehn, E.W. (2006). A highly conserved tyrosine of Tim-3 is phosphorylated upon stimulation by its ligand galectin-9. Biochem. Biophys. Res. Commun. *351*, 571–576.

van Rhenen, A., van Dongen, G.A., Kelder, A., Rombouts, E.J., Feller, N., Moshaver, B., Stigter-van Walsum, M., Zweegman, S., Ossenkoppele, G.J., and Jan Schuurhuis, G. (2007). The novel AML stem cell associated antigen CLL-1 aids in discrimination between normal and leukemic stem cells. Blood *110*, 2659–2666.

Wada, J., and Kanwar, Y.S. (1997). Identification and characterization of galectin-9, a novel beta-galactoside-binding mammalian lectin. J. Biol. Chem. *272*, 6078–6086.

Walter, M.J., Shen, D., Ding, L., Shao, J., Koboldt, D.C., Chen, K., Larson, D.E., McLellan, M.D., Dooling, D., Abbott, R., et al. (2012). Clonal architecture of secondary acute myeloid leukemia. N. Engl. J. Med. *366*, 1090–1098.

Wang, J., Iwasaki, H., Krivtsov, A., Febbo, P.G., Thorner, A.R., Ernst, P., Anastasiadou, E., Kutok, J.L., Kogan, S.C., Zinkel, S.S., et al. (2005). Conditional MLL-CBP targets GMP and models therapy-related myeloproliferative disease. EMBO J. *24*, 368–381.

Wang, Y., Krivtsov, A.V., Sinha, A.U., North, T.E., Goessling, W., Feng, Z., Zon, L.I., and Armstrong, S.A. (2010). The Wnt/beta-catenin pathway is required for the development of leukemia stem cells in AML. Science *327*, 1650–1653.

Welch, J.S., Ley, T.J., Link, D.C., Miller, C.A., Larson, D.E., Koboldt, D.C., Wartman, L.D., Lamprecht, T.L., Liu, F., Xia, J., et al. (2012). The origin and evolution of mutations in acute myeloid leukemia. Cell *150*, 264–278.

Yamaguchi, H., Hsu, J.L., and Hung, M.C. (2012). Regulation of ubiquitination-mediated protein degradation by survival kinases in cancer. Front. Oncol. *2*, 15.

Yamauchi, T., Takenaka, K., Urata, S., Shima, T., Kikushige, Y., Tokuyama, T., Iwamoto, C., Nishihara, M., Iwasaki, H., Miyamoto, T., et al. (2013). Polymorphic Sirpa is the genetic determinant for NOD-based mouse lines to achieve efficient human cell engraftment. Blood *121*, 1316–1325.

Yoshimoto, G., Miyamoto, T., Jabbarzadeh-Tabrizi, S., Iino, T., Rocnik, J.L., Kikushige, Y., Mori, Y., Shima, T., Iwasaki, H., Takenaka, K., et al. (2009). FLT3-ITD up-regulates MCL-1 to promote survival of stem cells in acute myeloid leukemia via FLT3-ITD-specific STAT5 activation. Blood *114*, 5034–5043.

Ysebaert, L., Chicanne, G., Demur, C., De Toni, F., Prade-Houdellier, N., Ruidavets, J.B., Mansat-De Mas, V., Rigal-Huguet, F., Laurent, G., Payrastre, B., et al. (2006). Expression of beta-catenin by acute myeloid leukemia cells predicts enhanced clonogenic capacities and poor prognosis. Leukemia *20*, 1211–1216.

Zhu, C., Anderson, A.C., Schubart, A., Xiong, H., Imitola, J., Khoury, S.J., Zheng, X.X., Strom, T.B., and Kuchroo, V.K. (2005). The Tim-3 ligand galectin-9 negatively regulates T helper type 1 immunity. Nat. Immunol. *6*, 1245–1252.